UV-B–Induced DNA Damage and Repair in the Mouse Lens

Rosana Mesa and Steven Bassnett

Department of Ophthalmology and Visual Sciences, Washington University School of Medicine, Saint Louis, Missouri

Correspondence: Steven Bassnett, Department of Ophthalmology and Visual Sciences, Washington University School of Medicine, 660 S. Euclid Avenue, Box 8096, St. Louis, MO 63110;
bassnett@vision.wustl.edu.

Submitted: June 21, 2013
Accepted: September 2, 2013

Citation: Mesa R, Bassnett S. UV-B–induced DNA damage and repair in the mouse lens. *Invest Ophthalmol Vis Sci.* 2013;54:6789–6797. DOI: 10.1167/iovs.13-12644

Purpose. Epidemiologic studies have linked UV-B exposure to development of cortical cataracts, but the underlying molecular mechanism(s) is unresolved. Here, we used a mouse model to examine the nature and distribution of DNA photolesions produced by ocular UV-B irradiation.

Methods. Anesthetized mice, eye globes, or isolated lenses were exposed to UV-B. Antibodies specific for 6-4 photoproducts (6-4 PPs) or cyclobutane pyrimidine dimers (CPDs) were used to visualize DNA adducts.

Results. Illumination of intact globes with UV-B–induced 6-4 PP and CPD formation in cells of the cornea, anterior iris, and central lens epithelium. Photolesions were not detected in retina or lens cells situated in the shadow of the iris. Photolesions in lens epithelial cells were produced with radiant exposures significantly below the minimal erythemal dose. Lens epithelial cells rapidly repaired 6-4 PPs, but CPD levels did not markedly diminish, even over extended postirradiation recovery periods in vitro or in vivo. The repair of 6-4 PPs did not depend on the proliferative activity of the epithelial cells, since the repair rate in the mitotically-active germinative zone (GZ) was indistinguishable from that of quiescent cells in the central epithelium.

Conclusions. Even relatively modest exposures to UV-B produced 6-4 PP and CPD photolesions in lens epithelial cells. Cyclobutane pyrimidine dimer lesions were particularly prevalent and were repaired slowly if at all. Studies on sun-exposed skin have established a causal connection between photolesions and so-called UV-signature mutations. If similar mechanisms apply in the lens, it suggests that somatic mutations in lens epithelial cells may contribute to the development of cortical cataracts.

Keywords: UV-B, cortical cataract, DNA damage

Solar irradiance at the top of Earth's atmosphere is 1361 W/m^2 (the solar constant)[1] and has a broad spectrum that peaks near the wavelength of yellow light (as predicted for a black body emitter with a surface temperature of approximately 5800° K). Less than 10% of solar radiation lies in the UV portion of the spectrum. The UV component is significantly attenuated as sunlight passes through the atmosphere. The highest energy UV photons, corresponding to the UV-C (100–280 nm) band are absorbed by ozone and other atmospheric gases and particulates. The UV-B portion of the spectrum lies between 280 and 315 nm. Short wavelength UV-B (280–290 nm) is almost completely absorbed by ozone but a significant fraction of long wavelength UV-B (290–315 nm) radiation penetrates to the planetary surface, along with a much larger proportion of UV-A (315–400 nm). Consequently, UV-A constitutes approximately 94% of terrestrial UV, and UV-B the remaining 6%.[2] The amount and spectral composition of UV radiation impinging on the corneal surface or intraocular tissues is influenced by many variables, including time of day (zenith angle), latitudinal location, surface reflectance properties, pupillary or squinting reflexes, and transmission characteristics of the various ocular media.[3] As a result, the actual irradiance of ocular structures is lower (by orders of magnitude) than standard meteorologic measurements of UV irradiance on a horizontal surface would suggest.

Ultraviolet B is a potent genotoxic agent and environmental mutagen.[4] Ultraviolet B photons are absorbed directly by DNA, leading to the production of two kinds of helix-distorting photolesions: cyclobutane pyrimidine dimers (CPDs) and 6-4 photoproducts (6-4 PPs).[5] Cyclobutane pyrimidine dimers and 6-4 PPs form between adjacent pyrimidine bases (cytosine or thymine). Photolesions in the DNA can result in C to T and CC to TT transitions during DNA replication.[6] These so-called "UV signature" mutations provide an indication of past sun exposure and are detected frequently in skin cancer.[6] Of the two types of primary photolesion, it is believed that CPDs are responsible for the majority (>80%) of mutations induced by UV-B irradiation of mammalian cells.[7,8]

The nucleotide excision repair (NER) pathway is particularly important in the repair of UV-induced photolesions and can be divided into two distinct subpathways: global genomic NER (GG-NER) and transcription-coupled NER (TC-NER).[9] The subpathways differ primarily in the manner by which the photolesions are detected initially. Global genomic NER identifies and repairs damage in silent genes, the nontranscribed strand of active genes, and in noncoding parts of the genome.[10] In GG-NER, photolesion-induced helix distortions are recognized by damage-sensors such as UV-damaged DNA binding protein (UV-DDB) and the XPC-Rad23B complex.[11] Mutations in genes encoding GG-NER proteins underlie xeroderma pigmentosum, an autosomal recessive condition characterized by an enormous increase (>1000-fold) in skin cancer risk.[12] Transcription-coupled NER is activated when RNA polymerase II stalls at, and thereby recognizes, a photo-

lesion on the transcribed strand of active genes. Downstream steps in NER, such as the incision, repair, and ligation processes that replace damaged DNA, are similar in GG-NER and TC-NER.[9]

The action spectra for many cytotoxic processes are heavily skewed toward shorter wavelengths.[13,14] As a result, although constituting only a small fraction of the total insolation, UV-B has a disproportionately large effect on ocular health. Chronic ocular exposure to solar UV-B radiation is a risk factor for cortical cataract, pinguecula, and pterygium, in addition to squamous cell carcinoma of the ocular surface.[15] With regard to cataract, an association between lifetime cumulative exposure to UV-B radiation and the development of cortical opacities was first identified in the classic study of watermen on the Chesapeake Bay,[16] and has been supported since by a number of epidemiologic investigations,[17] although the strength of the association has occasionally been questioned.[18] Interestingly, cortical opacities are most prevalent in the lower nasal quadrant of the lens,[19–22] perhaps due to the phenomenon of peripheral light focusing, through which temporal light rays are concentrated on this region of the lens.[23,24]

A number of studies have explored the link between UV-B and cortical cataracts, using both cell culture and animal models.[14,25–30] There are several pathways by which UV-B exposure could result in loss of lens transparency. Our laboratory is currently evaluating the hypothesis that UV-B–induced mutations contribute to cortical cataract development. As an initial step in this investigation we report here on UV-B–induced CPD and 6-4 PP production in lenses of wild-type mice, the protective effect afforded by the cornea and iris, and the capacity for DNA repair in various regions of the lens epithelium.

Materials and Methods

Animals

C57BL/6J mice (4–16-weeks old) were obtained from the Jackson Laboratory (Bar Harbor, ME). In some experiments, the eyes of anesthetized animals were irradiated with low doses (3 mJ/cm^2) of UV-B. For these experiments, mice were anesthetized with an intraperitoneal injection of ketamine (80 mg/kg body weight) and xylazine (6 mg/kg). In other cases, mice were killed by CO_2 inhalation and the eye enucleated. Intact globes or dissected lenses were then irradiated in vitro. Lenses were dissected from the eye through an incision in the posterior of the globe. All procedures conformed to the ARVO Statement for the Use of Animals in Ophthalmic and Vision Research and were approved by the Animal Studies Committee at Washington University.

UV-B Irradiation

For in vivo exposures, anesthetized animals were positioned such that the axis of the eye was aligned with the light source. One eye was irradiated with 3 mJ/cm^2 UV-B, the contralateral eye serving as an unirradiated control. This level of radiant exposure was chosen because it was below the minimal erythemal dose, well tolerated by the mice, and yet sufficient to produce detectable levels of photoproducts in the irradiated tissues. To examine the repair rate of UV-B–induced DNA photolesions, irradiated and unirradiated littermates were housed for 7 days following exposure. No opacities were found in the irradiated lenses 1 week after exposure. After 7 days, the nonirradiated animals were exposed to 3 mJ/cm^2 of UV-B and used as t equals 0 irradiated controls.

Intact globes or isolated lenses were placed in petri dishes containing a layer of 4% solidified low melting point agarose dissolved in Dulbecco's modified Eagle's Medium (DMEM)/F12 tissue culture medium (Gibco, Grand Island, NY). A hole of appropriate size was made in the agarose to accommodate the intact tissue. Tissue was positioned such that the anterior surface faced upward (i.e., toward the UV-B source). A small volume of PBS was added to cover the tissue surface and prevent dehydration during the irradiation protocol. To measure DNA repair rates in various regions of the lens epithelium, lenses were tilted at 45°, ensuring that the anterior and equatorial surfaces were exposed to the same irradiance. Samples were irradiated from above using a bank of six UV-B G8T5E fluorescence lamps (Sankyo Denki, Tokyo, Japan). Ultra violet B light sources generally emit a small amount of UV-C, which was removed using an acrylic filter (3.175-mm thick Plexiglas G-UVT; ACI Plastics, Inc., St. Louis, MO). The resulting emission spectrum of the illumination system was measured using a Black-comet-C-100 spectrometer (StellarNet, Inc., Tampa, FL) and ranged from 280 nm to 380 nm with a peak at 310 to 315 nm (Supplementary Fig. S1). The UV-B intensity at the sample surface was monitored continuously using an ILT 1700 radiometer equipped with a SED240/UVB/W detector fitted with a cosine correction diffuser (International Light Technologies, Peabody, MA). Measured irradiance at the sample varied slightly depending on the age of the lamps and ranged from 0.59 to 0.67 mW/cm^2. Following UV-B irradiation, samples were either fixed immediately and processed for immunofluorescence or placed in tissue culture to assess the capacity of the cells to repair UV-B–induced DNA damage. Tissue was cultured at 37°C under 5% CO_2 in DMEM/F12 tissue culture medium supplemented with insulin, transferrin, selenium, L-Glutamine, penicillin/streptomycin, fungizone, and 5% fetal bovine serum (FBS; Gibco, Grand Island, NY).

Immunofluorescence

Intact globes were fixed overnight in 4% paraformaldehyde/PBS and embedded in paraffin according to standard methods. Sagittal sections (5-μm thick) were dewaxed, rehydrated, and processed for antigen retrieval using citrate buffer (pH 6.0), at 95°C for 20 minutes. After permeabilization with 0.1% Triton X100, DNA was denatured by treatment with 2M HCl at room temperature for 30 minutes. Nonspecific staining was blocked with 5% normal goat serum in 1X Tris-buffered saline/0.1% Tween-20 for 1 hour at room temperature. Sections were then incubated overnight at 4°C with 1:500 dilution of mouse monoclonal anti-CPD (Cat # NMDND001; Cosmo Bio, Inc., Carlsbad, CA) or 1:300 dilution of mouse anti–6-4 PP (Cat # NMDND002, Cosmo Bio, Inc.).[31] Sections were washed and incubated for 2 hours at room temperature with Alexa488-conjugated goat anti-mouse (Invitrogen, Grand Island, NY). Nuclei were visualized using DRAQ 5 (Cell Signaling Technology, Inc., Danvers, MA). Unirradiated samples served as negative controls.

En face views of DNA damage in lens epithelial cells were obtained by dissecting epithelia from intact lenses following UV-B irradiation. Epithelia were carefully dissected from the lenses and pinned to the base of 35-mm petri dishes. Cyclobutane pyrimidine dimers and 6-4 PP photolesions were visualized in explanted epithelia using a modification of the labeling protocol described above for sectioned material. Epithelia were fixed in 4% paraformaldehyde for 20 minutes and permeabilized with 0.2% Triton X-100 for 12 minutes. DNA was denatured for 30 minutes in 2M HCl. Non-specific binding was minimized by incubation in blocking solution (5% FBS in PBS) for 30 minutes. The following dilutions of primary antibodies were used: 1:1800 anti-CPD, 1:1500 anti–6-4 PP, and 1:400 anti-proliferating cell

Investigative Ophthalmology & Visual Science

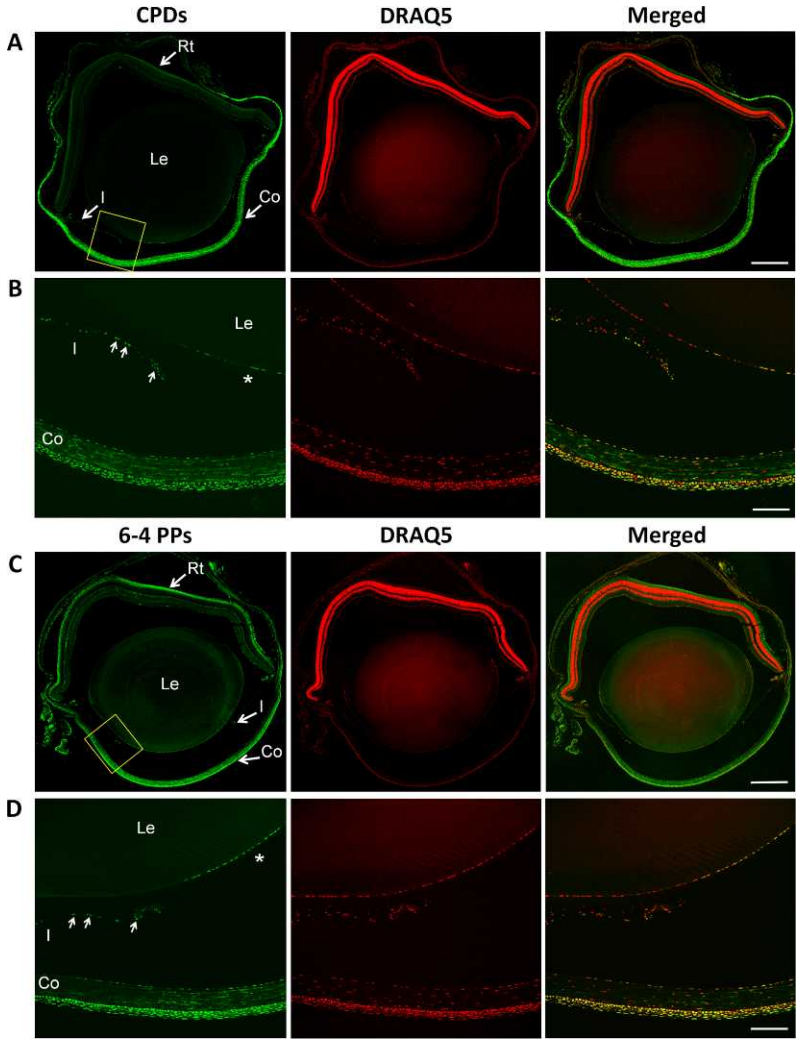

FIGURE 1. Distribution of photolesions following UV-B irradiation of intact globes. Mid-Sagittal paraffin sections of eyes from 2-month-old mice following irradiation with 500 mJ/cm^2 UV-B. Lesions were visualized with antibodies against CPDs or 6-4 PPs (*green*). Nuclei were counterstained with DRAQ5 (*red*). Strong CPD (**A**) and 6-4 PP (**C**) signals are detected in cornea, iris, and central lens epithelium. Boxed regions in (**A, C**) are shown at higher magnification in (**B, D**). Note the presence of CPD- and 6-4 PP-positive nuclei throughout the full thickness of the cornea. Nuclei at the anterior surface of the iris (*arrows*) and lens epithelial cells located in the pupillary space (*asterisk*) are labeled strongly. RT, retina; Le, lens; I, iris; Co, cornea. *Scale bars*: 0.5 mm (**A**, **C**); 100 μm (**B**, **D**).

nuclear antigen (PCNA, Cat # FL261; Santa Cruz Biotechnology, Inc., Santa Cruz, CA). The presence of PCNA was used to identify proliferating cells and delineate the germinative zone (GZ) of the lens.[32] Appropriate combinations of fluorescently-conjugated anti-mouse or anti-rabbit secondary antibodies (diluted 1:750) were used to visualize the tissue distribution of the primary antibodies. Nuclear DNA was counterstained with DRAQ5. Epithelia were coverslipped with mounting medium (Vectashield; Vector Laboratories, Burlingame, CA) and analyzed by confocal microscopy.

Image Acquisition and Analysis

Images were acquired on an Olympus FV1000 laser scanning confocal microscope (Olympus America, Inc., Center Valley, PA). Images stacks were collected using 10X (0.40 NA) air or 20X (0.85 NA) oil-immersion objectives. Alexa488, Alexa546, and DRAQ5 were excited using 488-, 546-, and 635-nm laser lines, respectively. Images were analyzed using Metamorph 7.77 software (Molecular Devices, Sunnyvale, CA). To quantify photolesion staining intensity, epithelial image stacks were collapsed to maximum intensity projections. The DRAQ5 image was used to create a mask defining the shape and position of each nucleus. The nuclear mask was applied to CPD or 6-4 PP channels and the average pixel intensity for each nucleus was determined after correcting for background fluorescence (the latter determined independently from unirradiated samples).

Statistical Analysis

Differences between groups were assessed by unpaired two-tailed *t*-test. Differences were considered significant at P less than 0.05.

RESULTS

Distribution of DNA Photolesions in Irradiated Ocular Tissue

It is well established that the cornea absorbs a significant fraction of the UV-B radiation impinging on the eye. The

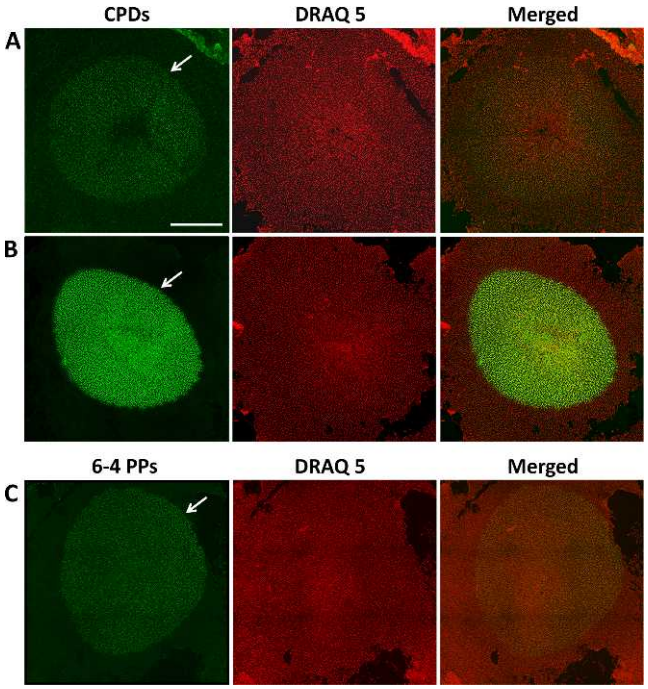

FIGURE 2. Analysis of photoproduct formation in the lens epithelium of irradiated eyes. Intact globes from 2-month-old mice were irradiated with UV-B at (**A**) 5 mJ/cm^2, (**B**) 250 mJ/cm^2, and (**C**) 50 mJ/cm^2. Lens epithelia were dissected, fixed and immunostained (*green*) with anti-CPD (**A**, **B**) and anti–6-4 PP (**C**). Nuclei were counterstained with DRAQ 5 (*red*). Both kind of photolesion are restricted to an elliptical region (*arrowed* in [**B**]) in the center of the epithelium. The size and shape of the elliptical region match the dimensions of the pupil. *Scale bar*: 0.5 mm.

human cornea, for example, absorbs more than 90% of UV-B[33] and UV-B intensity is reduced further as it crosses the anterior chamber.[34] The heavily-pigmented iris is expected to block much or all of the eccentric rays entering the eye, effectively shading epithelial cells near the lens equator from UV-B exposure. To examine the pattern of DNA damage caused by irradiation of the mouse eye, we exposed intact globes to UV-B in vitro. Antibodies specific for CPDs or 6-4 PPs were used to visualize the distribution of DNA photolesions at the surface of the irradiated globe and in intraocular tissues.

Globes were irradiated from the anterior aspect. As a result, CPDs and 6-4 PPs were abundant in superficial anterior structures, such as the cornea and the anterior portion of the sclera (Fig. 1). Photolesions were present throughout the full thickness of the cornea, including all layers of the epithelium, the stroma, and the endothelium. Photolesions were also detected in the nuclei of cells located in the anterior iris stroma. Lens epithelial cells located in the pupillary space were labeled strongly but the nuclei of peripheral lens epithelial cells and underlying fiber cells were not labeled. The peripheral lens cells were located in the shadow of the iris and the absence of photolesions from cells in this region indicated that the iris effectively screens those cells from UV-B irradiation, at least at the fluence used in the present experiments. Moderately high levels of fluorescence were also observed in the retina. However, most of the retinal staining was cytoplasmic rather than nuclear and probably represented non-specific antibody binding, since diffuse retinal fluorescence was also observed in unirradiated control eyes (Supplementary Fig. S2).

Histologic sections such as those shown in Figure 1 were useful for visualizing the intraocular distribution of photolesions following UV-B irradiation. However, even after antigen retrieval, the immunofluorescence signal was not strong in the sectioned material, necessitating the use of relatively high radiant exposures (500 mJ/cm^2) to cause detectable DNA damage. Moreover, the distribution of photolesions across the curved surface of the lens was difficult to quantify in sectioned material. To more sensitively detect DNA damage in the lens epithelium and better quantify the levels of CPD and 6-4 PP formation, we performed immunofluorescence analysis on lens epithelia that were explanted immediately after irradiation of the intact globe (Fig. 2). When the tissue was prepared in this fashion, CPDs were readily detected following radiant exposures of as little as 5 mJ/cm^2 (Fig. 2A). Higher doses of UV-B (50 mJ/cm^2) were necessary to detect 6-4 PPs (Fig. 2C), consistent with the notion that CPDs are the more commonly generated lesion after UV-B exposure.[7,8] Photolesions were present in nuclei lying within a sharply-defined elliptical region located in the center of the epithelium. The elliptical pattern was maintained even in eyes irradiated with relatively high doses (250 mJ/cm^2) of UV-B (Fig. 2B). The size and shape of the elliptical region closely matched the dimensions of the pupil, confirming that the iris effectively blocked UV-B–induced DNA damage to the peripheral lens epithelium.

To put these exposure data into perspective, we used our radiometer to measure outdoor UV-B irradiance on a clear June day in St. Louis, Missouri (located at 38° 38′ 07″ N). The measured UV-B irradiance was 0.07 mW/cm^2 at 1:00 PM (Supplementary Fig. S3). Under these conditions, UV-B radiant exposure values of 5 mJ/cm^2 and 50 mJ/cm^2 (Figs. 2A, 2C, respectively) would be reached in 71 and 714 seconds, respectively.

To gauge the UV-B transmittance of the mouse cornea, we compared the production of CPD photolesions in lens epithelial cell nuclei following exposure of either isolated lenses or intact globes with 5 mJ/cm^2 UV-B. Cyclobutane pyrimidine dimer immunofluorescence was quantified in the central regions of lens epithelia explanted from irradiated tissue (Fig. 3). In 1-month-old animals, lens CPD levels were reduced by approximately 80% when intact globes rather than isolated lenses were irradiated (Figs. 3A, 3B). These data suggest that the mouse cornea absorbs a significant fraction of the incident UV-B. A similar reduction in CPD levels was observed in experiments using tissue from older (4-month-old) mice, suggesting that corneal UV-B transmittance was relatively constant over time (Fig. 3C).

Differential Repair of CPDs and 6-4 PPs in the Lens Epithelium of UVB-Irradiated Eyes

Intact globes were irradiated with either 5 mJ/cm^2 (to generate CPDs) or 50 mJ/cm^2 (to generate 6-4 PPs) of UV-B. Lenses were then isolated and placed in organ culture for varying periods to assess the capacity of the epithelial cells to repair UV-B–induced photolesions (Fig. 4). As noted earlier, UV-B irradiation invariably resulted in DNA damage in lens epithelial cells situated in the pupillary space. Neither CPDs nor 6-4 PPs were detected in lens cells from unirradiated eyes nor in the peripheral epithelium of irradiated eyes.

The levels of CPDs remained relatively constant over the 24-hour postirradiation culture period (Figs. 4A, 4C). Indeed, there was a slight increase in the CPD immunofluorescence in culture, but that effect was not statistically significant. Some lenses were followed for 72 hours in culture, but no diminution in CPDs was detected, even over this extended in vitro culture period (data not shown). In contrast to CPDs, the levels of 6-4 PPs declined rapidly after irradiation (Figs. 4B, 4C). By 5.5 hours, 6-4 PP levels had fallen by more than 60% compared with measurements taken immediately after irradi-

Investigative Ophthalmology & Visual Science

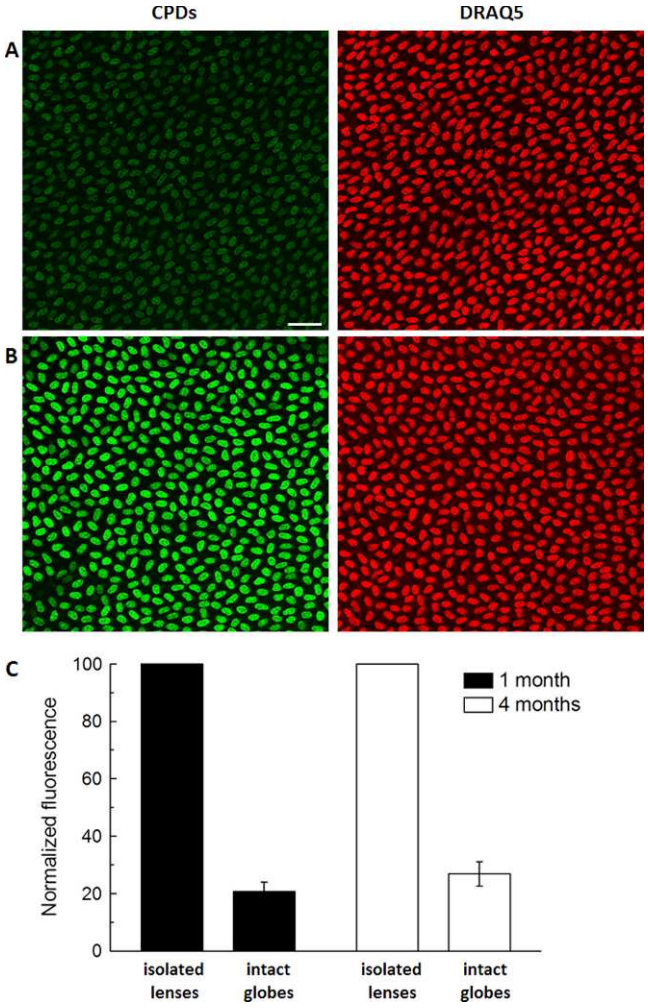

FIGURE 3. Cyclobutane pyrimidine dimer production in lens epithelia irradiated in situ or in isolation. Cyclobutane pyrimidine dimers were visualized by immunofluorescence and quantified using image analysis. The level of UV-B–induced CPDs in lens epithelial cell nuclei is significantly reduced when lenses are irradiated in situ (**A**) compared with irradiation in isolation (**B**). Quantitative analysis (**C**) suggests that lens CPD levels are reduced by 70% to 80% when intact globes rather than isolated lenses are irradiated. The shielding afforded by an intact globe is similar in 1-month-old and 4-month-old animals. Data represent the mean ± SEM of three to five independent experiments in each case. *Scale bar*: 25 μm.

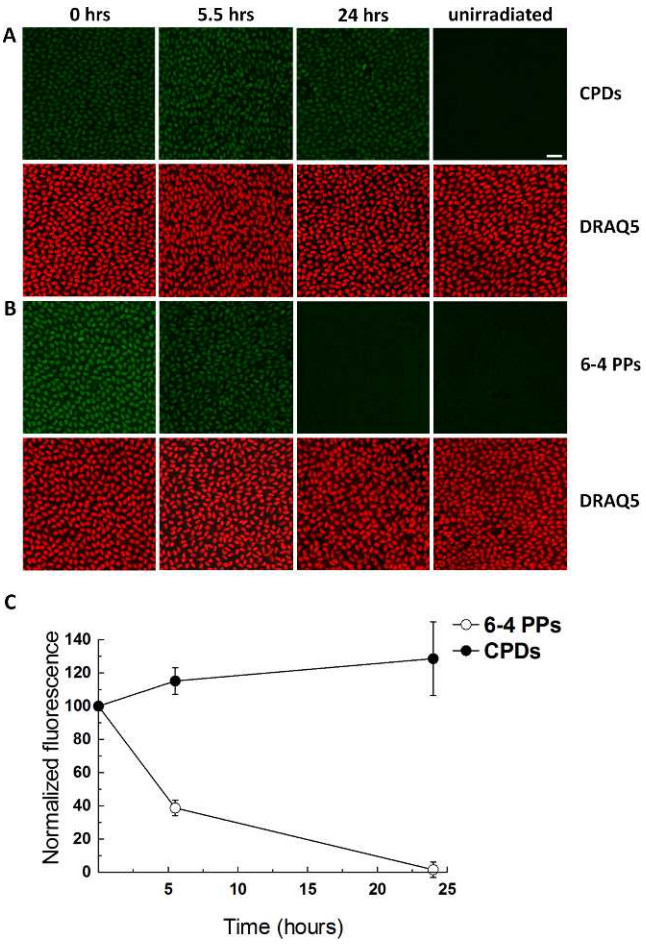

FIGURE 4. Differential repair of CPDs and 6-4 PPs in the lens epithelium of UVB-irradiated eyes. Intact globes from 1-month-old mice were irradiated with 5 mJ/cm^2 (**A**) or 50 mJ/cm^2 (**B**) of UV-B to induce formation of CPDs (**A**) or 6-4 PPs (**B**), respectively (*green*). Nuclear DNA (*red*) was visualized with DRAQ5 (*red*). Following irradiation, lenses were cultured for the periods shown, during which the levels of photolesions were quantified (**C**). Levels of 6-4 PPs return to baseline values after 24 hours in culture. In contrast, there is no reduction in CPDs over the culture period. Data represent the mean ± SEM of four to seven independent experiments for each time point. *Scale bar*: 25 μm.

ation (Fig. 4C). Twenty-four hours after irradiation, 6-4 PP levels in central lens epithelial cells had returned to baseline values and were indistinguishable from unirradiated samples or from epithelial nuclei located in the shadow of the iris. These data suggest that central lens epithelial cells in 1-month-old mice express robust mechanisms to repair UV-B–induced 6-4 PPs, but lack the capacity to repair UV-B–induced CPDs.

Ultraviolet B–induced CPD photolesions in the central lens epithelium were repaired slowly or not at all in vitro (Fig. 4C). To assess whether CPD repair capacity might be greater in vivo we irradiated live, anesthetized mice with low levels (3 mJ/cm^2) of UV-B and then examined the ability of lens epithelial cells to repair UV-B–induced CPDs (Fig. 5). The level of CPD photolesions in the central epithelial cells 1 week after UV-B exposure was greater than 70% of control values (Fig. 5C). Thus, even in vivo, the capacity of lens epithelial cells to repair UV-B–induced CPDs was low in comparison to their ability to repair 6-4 PPs.

6-4 PP Repair is Independent of Proliferative Activity

The ability of cells to recognize and repair UV-B–induced DNA damage is often correlated with their proliferative status. Deoxyribonucleic acid repair activity can be suppressed in terminally differentiated cells or cells arrested in G_0 of the cell cycle.[35] In vertebrate lenses, proliferative activity is compartmentalized, such that mitosis is restricted largely to the GZ, a swathe of epithelial cells that encircles the lens just above the equator.[36] We used the presence of PCNA to visualize the distribution of proliferating cells in the lens epithelium, thus, demarcating the border of the GZ (Fig. 6). Proliferating cell nuclear antigen–positive nuclei were extremely rare in the central zone (CZ) of the epithelium. In contrast, PCNA-positive nuclei were abundant in the GZ near the lens equator. To examine whether the repair capacity of lens epithelial cells was related to their proliferative activity, formation of 6-4 PPs was induced by exposure of isolated lenses to 5 mJ/cm^2 UV-B. The CZ and GZ regions were identified on the basis of PCNA

Investigative Ophthalmology & Visual Science

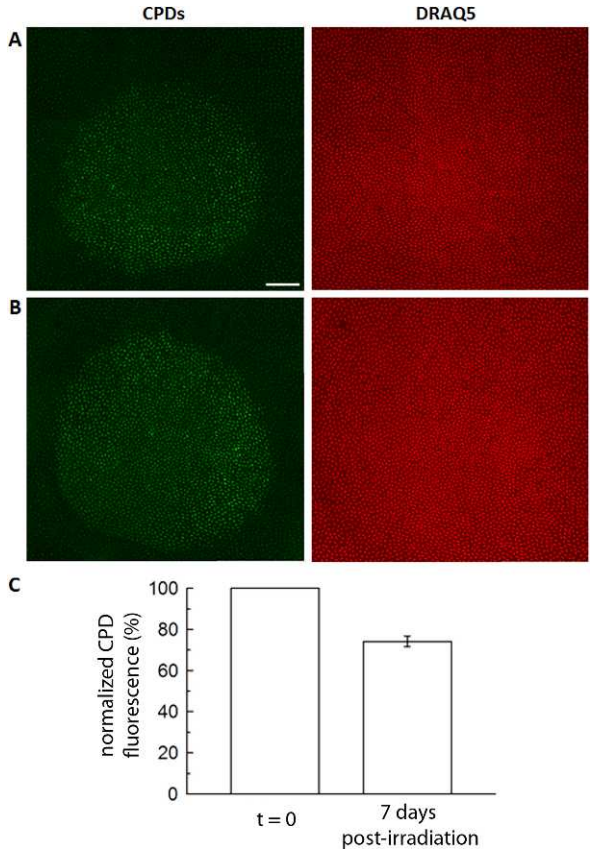

Figure 5. Ultraviolet-B–induced CPDs are not repaired over prolonged periods in vivo. Levels of CPDs (*green*) were quantified one week (**A**) after irradiation of 2-month-old mice with low level (3mJ/cm^2) UV-B and compared to values measured immediately after irradiation (**B**). There is a small (<30%) reduction in CPD levels one week after irradiation (**C**). Deoxyribonucleic acid was counterstained with DRAQ5 (*red*). *Scale bar*: 0.1 mm.

immunofluorescence (Fig. 6) and the relative rates of 6-4 PP repair in the two regions were computed (Fig. 7). By tilting the lens at 45°, it was possible to expose cells in the CZ and GZ to equal intensities of UV-B. As a result, comparable levels of 6-4 PPs were generated in the two regions initially (Fig. 7B). Six hours after irradiation, the 6-4 PP levels had fallen to approximately 70% of initial values. The fractional decrease in 6-4 PP levels in the CZ and GZ did not differ significantly (Fig. 7C), suggesting that the DNA repair rate was indistinguishable in the two regions, despite the marked difference in proliferative activity of cells in the two zones.

Discussion

Epidemiologic studies have indicated that UV-B exposure plays a role in the etiology of several ocular diseases including pterygium, pinguecula, and cortical cataract.[15] Deoxyribonucleic acid has an absorption maximum of 260 nm and DNA adducts can, therefore, be induced by direct absorption of UV-B photons. In contrast, UV-A radiation is absorbed only weakly by DNA and its putative ocular effects are therefore ascribed to indirect, photo-oxidative mechanisms.[37] Given the demonstrated role of UV-B in squamous and basal cell carcinoma of the epidermis, it is surprising that relatively few investigations have examined UV-B–induced DNA damage in the only other organ routinely exposed to the sun, the eye. Moreover, most studies to date have used cell-culture models.[14,38–40] In the current

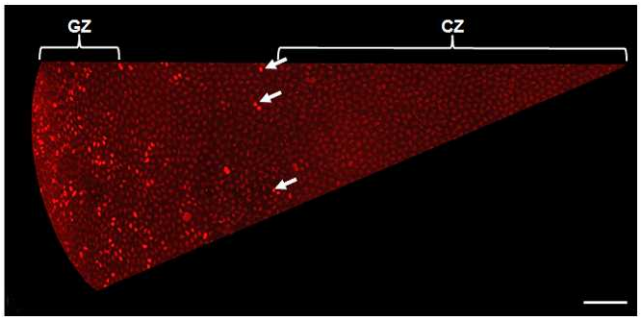

Figure 6. Regional distribution of proliferative activity in the lens epithelium. Mitotic cells (*arrows*) are visualized with PCNA staining in the lens epithelium of a 2-month-old mouse. Proliferating cells are localized to the GZ near the equatorial margin of the epithelium. Proliferating cells were rarely detected in the CZ of the epithelium. *Scale bar*: 0.1 mm.

investigation, irradiated ocular tissues were probed with antibodies against CPDs or 6-4 PPs.[31] The use of intact preparations rather than cell tissue culture models may more closely mimic the exposure patterns expected in vivo.

Exposure of the anterior surface of the ex vivo mouse eye to UV-B produced photolesions in nuclear DNA in both superficial and intraocular tissues. Sagittal sections revealed the presence of DNA-adducts throughout the full thickness of the cornea. These finding are consistent with earlier studies showing 6-4 PPs in rat corneas exposed to as little as 25 mJ/cm^2 of UV-B.[41] Similarly, CPDs were induced by UV-B exposure of the rabbit cornea.[42]

Corneal transmittance determines the potential impact of UV-B on intraocular tissues such as the lens. The cut off for corneal transmittance in the mouse is 280 to 285 nm,[25,43] somewhat shorter than the reported 290-nm cut off for rabbit[44] and human[25] corneas. The corneal transmittance of UV-B at 300 nm has been estimated to be 40% and 25% in albino and pigmented adult mice, respectively.[25,43] In the present study, sufficient UV-B penetrated the mouse cornea to produce photolesions in the central lens epithelium, even at radiant exposures as low as 3 mJ/cm^2. This is well below the minimal erythemal dose (MED), which, in mice, ranges from 50 to 470 mJ/cm^2, depending on the strain and the nature of the UV-B source.[45,46] Both CPDs and 6-4 PPs were produced, although CPDs were the more abundant lesion. The level of lens CPDs increased by 4- to 5-fold when the isolated lens rather than the intact eye was irradiated with UV-B, confirming that, in mice, the cornea absorbs a significant fraction of the incident UV-B. Cyclobutane pyrimidine dimers and 6-4 PPs were also detected in cells at the anterior surface of the iris but not in the peripheral lens epithelium, which is located in the shadow of the iris. Thus, at the irradiance used here, the thin but heavily-pigmented iris blocked enough of the incident UV-B to prevent photolesions in the proliferatively-active GZ of the lens epithelium. A similar shielding phenomenon has been reported in the rabbit eye.[42]

The capacity of lens epithelial cells to repair UV-B–induced damage to DNA has been examined in several studies. For example, extended lifespan human lens epithelium (HLE) B-3 cells were able to repair both 6-4 PPs and CPDs after UV-B exposure.[40] Twenty-four hours after UV-B exposure of HLE B-3 cells, 95% of 6-4 PPs were repaired but only 50% of CPDs. The observation that 6-4 PPs were removed more rapidly than CPDs is a consistent finding in many cell types.[47] The difference in repair rate may be attributed to the fact that 6-4 PPs cause a greater distortion in the DNA helix than CPDs and, therefore, have a higher affinity for repair factors in the nucleotide

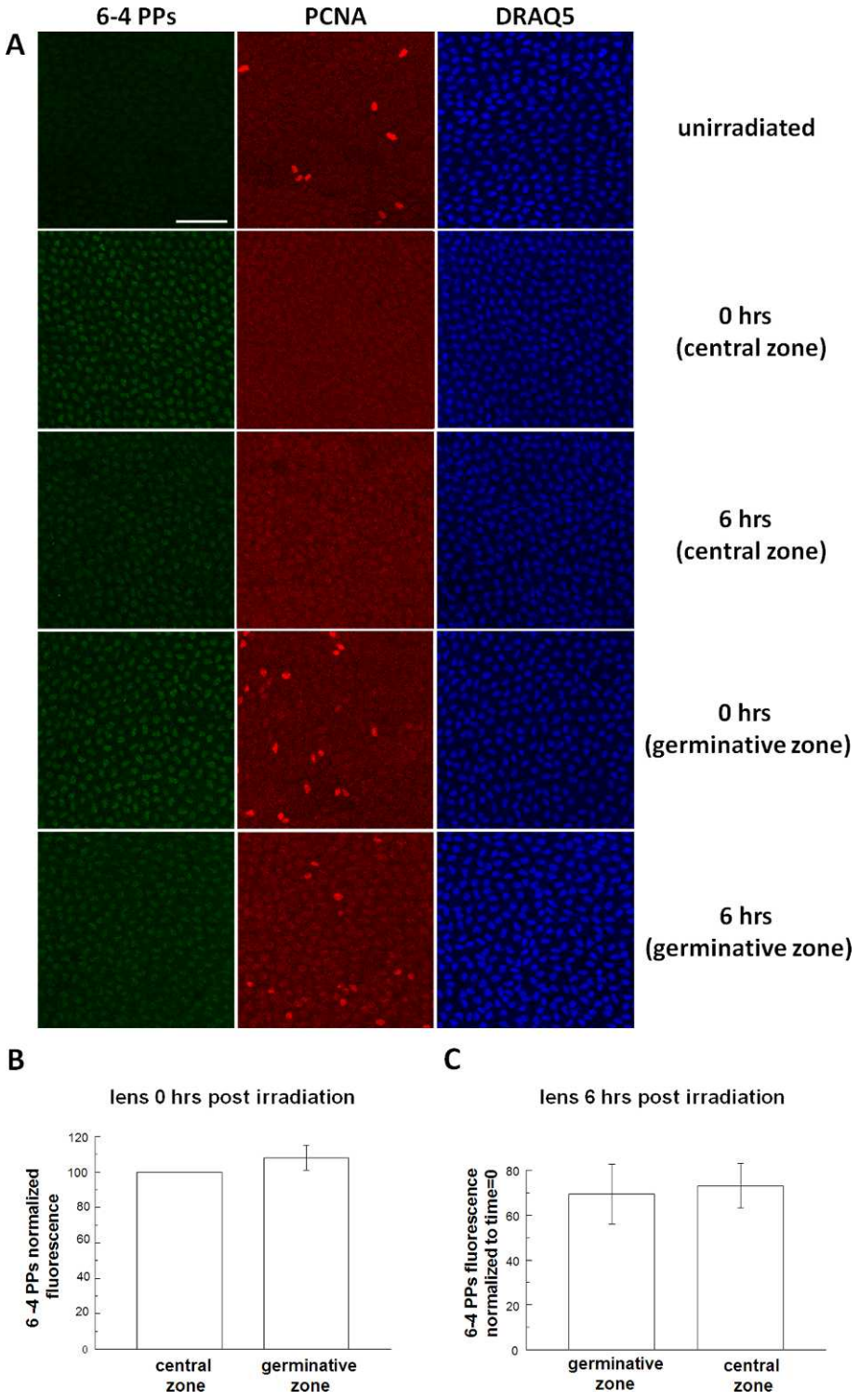

Figure 7. Deoxyribonucleic acid repair capacity is not related to proliferative activity. Lenses were exposed to UV-B (5 mJ/cm^2) to induce 6-4 PP formation and then placed in culture to assess the capacity of cells in the CZ and GZ to repair UV-B–induced DNA damage. (**A**) Photolesions were visualized with anti–6-4 PPs (*green*). The distribution of mitotic cells was determined by PCNA immunofluorescence (*red*) and nuclei were counterstained with DRAQ5 (*blue*). 6-4 PPs levels are initially comparable in the two regions (**B**) and subsequently decline at similar rates (**C**). After 6 hours the levels had fallen to approximately 70% of the value at $t = 0$. *Scale bar*: 50 μm.

excision repair pathway.[48] In the current study, 6-4 PPs were almost completely removed from lens epithelial cells during the 24-hour postirradiation culture period. Although relatively rapid, these kinetics are not exceptional and are comparable to rates in astrocytes and neurons,[49] for example, and slower than cultured fibroblasts.[50] In contrast to 6-4 PPs, UV-B–induced CPD photolesions persisted in the lens epithelium with little or no recovery over the 24-hour postirradiation culture period in vitro. This observation was subsequently confirmed in vivo, where little (≈30%) recovery was noted seven days after

irradiation. Global genomic NER is involved in the removal of UV photoproducts, particularly CPDs.[51] A key initial step in GG-NER is recognition of the CPD lesion by the UV-damaged DNA binding protein (UV-DDB) complex. The UV-DDB complex is a heterodimer composed of a large subunit, damage-specific DNA binding protein 1 (DDB1), and a small subunit, DDB2. Significantly, expression of DDB2 in many murine tissues, especially epidermis,[52] is low. This is associated, in rodents, with a general deficit in GG-NER removal of CPDs, which can be reversed by transgenic expression of DBB2.[53]

The rate of photolesion removal can also be influenced by the proliferative status of the cells and is often reduced in terminally differentiated cells or cells arrested in the G_0 stage of the cell cycle.[35] Were this true in the lens, DNA repair rates in the peripheral (mitotically-active) epithelium might be expected to exceed those in the central (mitotically-quiescent) region. However, no such difference was found. The DNA repair capacity of the lens epithelial cells was independent of epithelial location.

In summary, exposure of mouse ocular tissue to levels of UV-B considerably below the MED threshold resulted in the generation of 6-4 PP and CPD photolesions in the central lens epithelium. The epithelial cells were able to repair 6-4 PPs but lacked the capacity to repair CPDs. The persistence of DNA lesions may predispose mouse lens cells to UV-induced somatic mutations. Unlike mice, humans are a diurnal species and, consequently, it is likely that human lens epithelial cells have more robust DNA repair mechanisms. Moreover, the human cornea, being considerably thicker than that of the mouse, is also expected to block a greater fraction of the incident UV-B. Consequently, it is difficult to predict whether high levels of UV-B–induced damage might accumulate in the human lens epithelium. There have been few studies on this topic, but in one recent analysis of DNA damage in human capsulotomy specimens, CPDs were detected, in addition to relatively high levels of oxidized purines.[54] It is not known whether UV-B–induced DNA damage in the human lens epithelium results in UV-signature mutations, but with advances in DNA sequencing technology, it should soon be possible to determine this directly.

Acknowledgements

Supported by National Institutes of Health Grants EY09852 (SB), Core Grant for Vision Research P30 EY02687, and an unrestricted grant to the Department of Ophthalmology and Visual Sciences from Research to Prevent Blindness.

Disclosure: **R. Mesa**, None; **S. Bassnett**, None

References

1. Kopp G, Lean JL. A new, lower value of total solar irradiance: evidence and climate significance. *Geophys Res Lett*. 2011;38. doi:10.1029/2010GL045777.
2. Diffey BL. Sources and measurement of ultraviolet radiation. *Methods*. 2002;28:4–13.
3. Sliney DH. Intraocular and crystalline lens protection from ultraviolet damage. *Eye Contact Lens*. 2011;37:250–258.
4. Lucas R, McMichael T, Smith W, Armstrong B. *Solar Ultraviolet Radiation: Global Burden of Disease From Solar Ultraviolet Radiation*. Geneva: World Health Organization; 2006.
5. Beukers R, Eker AP, Lohman PH. 50 years thymine dimer. *DNA Repair (Amst)*. 2008;7:530–543.
6. Brash DE, Rudolph JA, Simon JA, et al. A role for sunlight in skin cancer: UV-induced p53 mutations in squamous cell carcinoma. *Proc Natl Acad Sci U S A*. 1991;88:10124–10128.
7. Besaratinia A, Yoon JI, Schroeder C, Bradforth SE, Cockburn M, Pfeifer GP. Wavelength dependence of ultraviolet radiation-induced DNA damage as determined by laser irradiation suggests that cyclobutane pyrimidine dimers are the principal DNA lesions produced by terrestrial sunlight. *FASEB J*. 2011; 25:3079–3091.
8. You YH, Lee DH, Yoon JH, Nakajima S, Yasui A, Pfeifer GP. Cyclobutane pyrimidine dimers are responsible for the vast majority of mutations induced by UVB irradiation in mammalian cells. *J Biol Chem*. 2001;276:44688–44694.
9. Friedberg EC. How nucleotide excision repair protects against cancer. *Nat Rev Cancer*. 2001;1:22–33.
10. Nouspikel T. DNA repair in mammalian cells: nucleotide excision repair: variations on versatility. *Cell Mol Life Sci*. 2009;66:994–1009.
11. Sugasawa K, Ng JM, Masutani C, et al. Xeroderma pigmentosum group C protein complex is the initiator of global genome nucleotide excision repair. *Mol Cell*. 1998;2:223–232.
12. DiGiovanna JJ, Kraemer KH. Shining a light on xeroderma pigmentosum. *J Invest Dermatol*. 2012;132:785–796.
13. Oriowo OM, Cullen AP, Chou BR, Sivak JG. Action spectrum and recovery for in vitro UV-induced cataract using whole lenses. *Invest Ophthalmol Vis Sci*. 2001;42:2596–2602.
14. Andley UP, Lewis RM, Reddan JR, Kochevar IE. Action spectrum for cytotoxicity in the UVA- and UVB-wavelength region in cultured lens epithelial cells. *Invest Ophthalmol Vis Sci*. 1994;35:367–373.
15. Cullen AP. Ozone depletion and solar ultraviolet radiation: ocular effects, a United Nations environment programme perspective. *Eye Contact Lens*. 2011;37:185–190.
16. Taylor HR, West SK, Rosenthal FS, et al. Effect of ultraviolet radiation on cataract formation. *N Engl J Med*. 1988;319:1429–1433.
17. McCarty CA, Taylor HR. A review of the epidemiologic evidence linking ultraviolet radiation and cataracts. *Dev Ophthalmol*. 2002;35:21–31.
18. Dolin PJ, Johnson GJ. Solar ultraviolet radiation and ocular disease: a review of the epidemiological and experimental evidence. *Ophthalmic Epidemiol*. 1994;1:155–164.
19. Sasaki H, Kawakami Y, Ono M, et al. Localization of cortical cataract in subjects of diverse races and latitude. *Invest Ophthalmol Vis Sci*. 2003;44:4210–4214.
20. Abraham AG, Cox C, West S. The differential effect of ultraviolet light exposure on cataract rate across regions of the lens. *Invest Ophthalmol Vis Sci*. 2010;51:3919–3923.
21. Schein OD, West S, Munoz B, et al. Cortical lenticular opacification: distribution and location in a longitudinal study. *Invest Ophthalmol Vis Sci*. 1994;35:363–366.
22. Rochtchina E, Mitchell P, Coroneo M, Wang JJ, Cumming RG. Lower nasal distribution of cortical cataract: the Blue Mountains Eye Study. *Clin Experiment Ophthalmol*. 2001; 29:111–115.
23. Coroneo MT. Albedo concentration in the anterior eye: a phenomenon that locates some solar diseases. *Ophthalmic Surg*. 1990;21:60–66.
24. Coroneo MT, Muller-Stolzenburg NW, Ho A. Peripheral light focusing by the anterior eye and the ophthalmohelioses. *Ophthalmic Surg*. 1991;22:705–711.
25. Dillon J, Zheng L, Merriam JC, Gaillard ER. The optical properties of the anterior segment of the eye: implications for cortical cataract. *Exp Eye Res*. 1999;68:785–795.
26. Hightower K, McCready J. The role of calcium in UVB-induced damage in irradiated ocular lenses. *Photochem Photobiol*. 1997;65:155–160.
27. Hightower KR, McCready JP, Borchman D. Membrane damage in UV-irradiated lenses. *Photochem Photobiol*. 1994;59:485–490.

28. Hightower KR, Reddan JR, McCready JP, Dziedzic DC. Lens epithelium: a primary target of UVB irradiation. *Exp Eye Res*. 1994;59:557–564.
29. Reddy GB, Bhat KS. Synergistic effect of UVB radiation and age on HMPS enzymes in rat lens homogenate. *J Photochem Photobiol B*. 1998;43:56–60.
30. Reddy GB, Bhat KS. UVB irradiation alters the activities and kinetic properties of the enzymes of energy metabolism in rat lens during aging. *J Photochem Photobiol B*. 1998;42:40–46.
31. Mori T, Nakane M, Hattori T, Matsunaga T, Ihara M, Nikaido O. Simultaneous establishment of monoclonal antibodies specific for either cyclobutane pyrimidine dimer or (6-4) photoproduct from the same mouse immunized with ultraviolet-irradiated DNA. *Photochem Photobiol*. 1991;54:225–232.
32. Hall PA, Levison DA, Woods AL, et al. Proliferating cell nuclear antigen (PCNA) immunolocalization in paraffin sections: an index of cell proliferation with evidence of deregulated expression in some neoplasms. *J Pathol*. 1990;162:285–294.
33. Zigman S. Ocular light damage. *Photochem Photobiol*. 1993; 57:1060–1068.
34. Zigman S. Environmental near-UV radiation and cataracts. *Optom Vis Sci*. 1995;72:899–901.
35. Hyka-Nouspikel N, Lemonidis K, Lu WT, Nouspikel T. Circulating human B lymphocytes are deficient in nucleotide excision repair and accumulate mutations upon proliferation. *Blood*. 2011;117:6277–6286.
36. Harding CV, Hughes WL, Bond VP, Schork P. Autoradiographic localization of tritiated thymidine in wholemount preparations of lens epithelium. *Arch Ophthalmol*. 1960;63:58–65.
37. Zigman S. Lens UVA photobiology. *J Ocul Pharmacol Ther*. 2000;16:161–165.
38. Kleiman NJ, Wang RR, Spector A. Ultraviolet light induced DNA damage and repair in bovine lens epithelial cells. *Curr Eye Res*. 1990;9:1185–1193.
39. Sidjanin D, Zigman S, Reddan J. DNA damage and repair in rabbit lens epithelial cells following UVA radiation. *Curr Eye Res*. 1993;12:773–781.
40. Andley UP, Song Z, Mitchell DL. DNA repair and survival in human lens epithelial cells with extended lifespan. *Curr Eye Res*. 1999;18:224–230.
41. Estil S, Olsen WM, Huitfeldt HS, Haaskjold E. UVB-induced formation of (6-4) photoproducts in the rat corneal epithelium. *Acta Ophthalmol Scand*. 1997;75:120–123.
42. Mallet JD, Rochette PJ. Ultraviolet light-induced cyclobutane pyrimidine dimers in rabbit eyes. *Photochem Photobiol*. 2011; 87:1363–1368.
43. Henriksson JT, Bergmanson JP, Walsh JE. Ultraviolet radiation transmittance of the mouse eye and its individual media components. *Exp Eye Res*. 2010;90:382–387.
44. Walsh JE, Bergmanson JP, Koehler LV, Doughty MJ, Fleming DP, Harmey JH. Fibre optic spectrophotometry for the in vitro evaluation of ultraviolet radiation (UVR) spectral transmittance of rabbit corneas. *Physiol Meas*. 2008;29:375–388.
45. Reeve VE, Boehm-Wilcox C, Bosnic M, Reilly WG. Differential photoimmunoprotection by sunscreen ingredients is unrelated to epidermal cis urocanic acid formation in hairless mice. *J Invest Dermatol*. 1994;103:801–806.
46. Rebel H, Mosnier LO, Berg RJ, et al. Early p53-positive foci as indicators of tumor risk in ultraviolet-exposed hairless mice: kinetics of induction, effects of DNA repair deficiency, and p53 heterozygosity. *Cancer Res*. 2001;61:977–983.
47. Mitchell DL, Haipek CA, Clarkson JM. (6-4) Photoproducts are removed from the DNA of UV-irradiated mammalian cells more efficiently than cyclobutane pyrimidine dimers. *Mutat Res*. 1985;143:109–112.
48. Buterin T, Hess MT, Gunz D, Geacintov NE, Mullenders LH, Naegeli H. Trapping of DNA nucleotide excision repair factors by nonrepairable carcinogen adducts. *Cancer Res*. 2002;62: 4229–4235.
49. Yamamoto A, Nakamura Y, Kobayashi N, et al. Neurons and astrocytes exhibit lower activities of global genome nucleotide excision repair than do fibroblasts. *DNA Repair (Amst)*. 2007; 6:649–657.
50. Nishiwaki Y, Kobayashi N, Imoto K, et al. Trichothiodystrophy fibroblasts are deficient in the repair of ultraviolet-induced cyclobutane pyrimidine dimers and (6-4) photoproducts. *J Invest Dermatol*. 2004;122:526–532.
51. Yeh JI, Levine AS, Du S, et al. Damaged DNA induced UV-damaged DNA-binding protein (UV-DDB) dimerization and its roles in chromatinized DNA repair. *Proc Natl Acad Sci U S A*. 2012;109:E2737–E2746.
52. Tan T, Chu G. p53 Binds and activates the xeroderma pigmentosum DDB2 gene in humans but not mice. *Mol Cell Biol*. 2002;22:3247–3254.
53. Alekseev S, Kool H, Rebel H, et al. Enhanced DDB2 expression protects mice from carcinogenic effects of chronic UV-B irradiation. *Cancer Res*. 2005;65:10298–10306.
54. Osnes-Ringen O, Azqueta AO, Moe MC, et al. DNA damage in lens epithelium of cataract patients in vivo and ex vivo [published online ahead of print September 20, 2012]. *Acta Ophthalmol*. doi:10.1111/j.1755-3768.2012.02500.x.

Investigative Ophthalmology & Visual Science